International Journal of Applied Chemistry.
ISSN 0973-1792 Volume 12, Number 3 (2016) pp. 359-374

http://www.ripublication.com

Chiral Surfaces Formed by Uracil, 5-Hydroxy-6-Methyluracil and Melamine Supramolecular Structures

Vladimir Yu. Gus'kov, Yulia Yu. Gainullina, Darya A. Suhareva, Artem V. Sidel'nikov and Florida Kh. Kudasheva

Bashkir State University, Ufa, Russia.

Abstract

In this work the phenomenon of supramolecular chirality of uracil, 5-hydroxy-6-methyluracil and melamine achiral molecules was used to obtain novel chiral surfaces. Modifiers were impregnated on the inert solid support or adsorbent and packed in a stainless steel column. The enantiomers of menthol, camphene, limonene and camphor and their racemates were used as probes. Using gas chromatography, the specific retention volumes, separation factors and thermodynamic functions of enantiomer adsorption were determined. It was shown that the adsorbents tested were selective for all enantiomers studied in a broad temperature range. Separation factors strongly depended on the column temperature. The enantioselectivity phenomenon is depending on the difference in the internal energy and entropy of enantiomer adsorption on the supramolecular structure surface. The last most likely was caused by the mirror-symmetry breaking during the supramolecular structures forming, which leads to macroscopic chirality. It is established, that mirror-symmetry breaking phenomenon was caused by stirring.

Keywords: supramolecular chirality, chiral surfaces, enantiomers, uracil, stirring

1. INTRODUCTION

The nanoscale-ordered material design is one of the major challenges in modern surface chemistry. Among other such materials, chiral surfaces attract researches because of it applicability in biological and chemical sensors construction, as well as in the field of electrocatalysis and electronic and optical materials [1-3]. The most widespread chiral surfaces are based on cyclodextrins, which were used for enantiomer separation for the first time by Kościelski [4]. A great deal of surfaces with cyclodextrins as chiral selectors have been used in electrochemical sensors [5-7]

and in separation science [8, 9]. However, despite many advantages, in some cases enantioselectivity and stability (include temperature stability) are not satisfactory for such surfaces. In recent years efforts to increase selectivity have concentrated on modifying existing cyclodextrin surfaces, by chemical linking with different functional groups or by using mixed surfaces cyclodextrin-modifier [10-13]. Sometimes liquid crystals have been used as modifiers [14]. Yet the problems of relatively high volatility and low stability have not been completely solved. Therefore, in order to achieve the required stability and enantioselectivity, the development of new chiral surfaces with fundamentally novel chiral selection is topical. Recently new promising types of surfaces, based on ionic liquids [15], porous polymers with molecular imprints [16] and single-walled carbon nanotubes encapsulated into different polymer-based monolithic backbones [17] have appeared. But the base of chiral recognition is still untouched.

Any chiral recognition required surface homochirality or at least the excess of one enantiomer. The described above surfaces have one similar property: in all cases the enantiomers separations were based on surface *molecules* homochirality/enantiomer excess. But the chirality phenomenon is not limited by *the molecular chirality* only. During the last ten years *the supramolecular chirality* phenomenon was intensively studied [18-20]. Supramolecular chirality arises from the non-symmetric spatial arrangement of components in those assemblies formed via noncovalent interactions. The chiral supramolecular assemblies are widely used in the fields of enantioselective separation and catalysis, chiral molecular recognition, and nonlinear optical materials [21]. Supramolecular chirality strongly related to both the chirality of the molecular components and their assembly manner [22]. The most fascinating in supramolecular chirality is the possibility for either chiral or achiral molecules to assembly into chiral nano/microstructures through non-covalent bonds. [18, 22-43]. In several cases the supramolecular chirality was induced by the formation of a host–guest supramolecular complex [43] or supramolecular self-assemblies [21, 29, 44, 45] between chiral and achiral molecules. But the most attractive and exciting is the formation of chiral 1D, 2D or 3D supramolecular structures only by the achiral molecules. This phenomenon was observed both in the case of some external conditions influence and without it. As external force, that inducing or enhancing supramolecular chirality, the using of polarized light [19, 26, 41, 46] optically pure solvent [19, 20, 30, 39] temperature [22, 34] and even stirring [47] were proposed. At the same time, a few papers report about the spontaneously formed supramolecular chirality from the achiral molecules [14, 23-28, 31, 35-38, 40, 48-50]. From the theoretical point of view, the supramolecular structure forming should have the left- and right-handed clusters in equal amounts and become overall racemic, showing only local chirality but no macroscopic optical activity, leading to unsuitability for enantiomers separation. But for some supramolecular structures described the overall chirality observed [22, 25, 26, 30, 31, 34-36, 40]. Such macroscopic chirality was determined even in the solution [30] and in the crystal [40]. Moreover, it was shown, that such structures are capable of chiral selection [51].

So, such data inspired us to try uracil, 5-hydroxy-6-methyluracil (HMU) and melamine supramolecular 2D-structures to construct novel nanoscale-ordered sufaces.

The molecules of these substances are not chiral, but their supramolecular structures on the solid surface have R- and S-chiral domains [14, 23]. Yet the enantiomer excess or racemic nature of such structures is not determined at the present. Therefore it is interesting to ascertain whether the surfaces, based on uracil, HMU and melamine, can separate enantiomers in chromatographic conditions.

2. MATERIALS AND METHODS

2.1. Packed column preparation

The inert solid support for gas–liquid chromatography Inerton N (Chemapol, Prague, Czech Republic) was used. Graphitized carbon black Carbopack C (Sigma-Aldrich, USA) and porous polymer Polysorb-1 (Russia) were used. Uracil (Avilon-CompanyChim, Moscow, Russia) and melamine (Agropromservis, Moscow, Russia) were used. HMU was obtained from the Institute of Organic Chemistry (Ufa, Russia). Supramolecular structure impregnation was performed according to reference [52]. The amount of impregnated modifier was 1% of the mass of the solid support, 10% of the mass of the Carbopack C and 5% of the mass of the Polysorb-1. All adsorbents obtained were packed in stainless steel columns measuring 1000 x 3 mm.

2.2. Analytes

D-limonene (97%, Sigma-Aldrich, Milwaukee, USA), L-limonene (96%, Sigma-Aldrich, Milwaukee, USA), D-menthol (99.9%, Sigma-Aldrich, Milwaukee, USA), DL-menthol (99.4%, Acros organics, Geel, Belgium), L-menthol (99.4%, Sigma-Aldrich, Milwaukee, USA), L-camphene (80%, Alfa Aesar, Karlsruhe, Germany), D-camphene (90%, Merck, Darmstadt, Germany), D-camphor (98.8%, Acros organics, Geel, Belgium), L-camphor (95.8%, Acros organics, Geel, Belgium) and DL-camphor (96%, Acros organics, Geel, Belgium) and 2-butanol (99.5%, Sigma-Aldrich, Milwaukee, USA) were used. Limonenes and 2-butanol were injected as pure compounds; menthols, camphenes and camphor were injected as 0.1 g/ml solutions in pentane. The choice of solvent was governed by the necessity of eliminating overlapping solvent and analyte peaks. For both enantiomers the amount injected was similar.

2.3. Gas chromatography

A Tswett 500M gas chromatograph (Tswett, Dzerginsk, Russia) equipped with flame ionization detector was used. The column temperature range is from 40 to 150 ˚C. The nitrogen carrier gas flow rate was 10 ml/min. Such a flow rate roughly corresponds with the minimum on the van Deemter plot.

2.4. Calculations

The specific retention volumes ($V^{\circ}_{g(T)}$), ml/g, were calculated by the expression:

$$V^{0}_{g(T)} = j\,\frac{(t_R - t_M)\omega}{m} \quad (1)$$

where j – the James-Martin compressibility factor; t_R – the retention time, min; t_M – the retention time of substances not retained in the adsorbent bed, min; ω – the flow

rate of the carrier gas, ml/min; m – the total mass of adsorbent in the column, g. At the flow rate used, peak desorption branches were superimposed, and the specific retention volumes were independent of the flow rate. It allowed the adsorption processes in the column to be considered as close to ideal linear chromatography, making it possible to equate $V°_{g(T)}$ with the adsorption–desorption equilibrium constants (Henry's constants):

$$H_{a,c}^{0} = V_{g(T)}^{0} \quad (2)$$

1.

From the $V°_{g(T)}$ vs. 1/T dependence,

$$lnV_{g(T)}^{0} = -\frac{\Delta U}{RT} + \frac{\Delta S}{R} + 1 \quad (3)$$

differential isosteric internal energy (−ΔU, kJ/mol) and entropy (−ΔS, J/(mol K)) of adsorption were calculated.

From,

$$\alpha = \frac{V_{g(T)1}^{0}}{V_{g(T)2}^{0}} \quad (4)$$

the separation factor α was calculated.

3. RESULTS AND DISCUSSION

3.1. Enantioselectivity of the studied adsorbents

In tables 1–4 the specific retention volumes and the separation factors (α) for camphene, limonene, camphor and menthol at the different temperatures are listed. The lower temperature limit was conditioned by sufficient peak broadening caused by strong analyte adsorption on the adsorbent surface. The upper limit was governed by the overlapping of the analyte and solvent peaks. As can be seen from the tables, all supramolecular structure-based adsorbents are capable of separating enantiomers. The enantioselectivity was observed in a broad temperature range. The best selectivity for camphenes was achieved on the column with melamine at 60 and 80 °C (α=2.36±0.21 and 2.67±0.12 respectively). At other temperatures the selectivity of melamine supramolecular structure was also relatively high. The adsorbent based on uracil showed high enantioselectivity with respect to camphenes at T=40–50 and 60–75 °C. Under those conditions, the maximal separation factor was 1.65±0.19. Limonene on uracil had the best separation at 55 °C. On HMU, the separation factors for limonene had smaller values and reached a maximum at 50 °C. The maximum enantioselectivity was observed with limonene on the column with melamine at 40–45 °C. Unlike limonene, camphor on melamine had the best separation at 65–80 °C, although an even higher separation factor was observed at 85 °C. In respect to the menthol polar molecule the highest separation factors were achieved on uracil at 70 °C (α=2.35±0.21), 55 °C (α=2.04±0.26) and 50 °C (α=1.94±0.09). For surfaces with melamine the menthol separation was slightly worse — the highest α value was 1.83±0.11 at 80 °C.

One can conclude that from all the adsorbents studied those based on HMU had the least enantioselectivity. Adsorbents based on uracil and melamine possessed good selectivity with respect to the polar molecules menthol and camphor, as well as to nonpolar limonene and camphene. It is noticeable that on HMU menthol, camphene and camphor have very large values for $V°_{g(T)}$. The ability of the HMU supramolecular structure to sufficiently adsorb both polar and nonpolar molecules was described in [52] for a number of organic substances. Probably this phenomenon was caused by the presence of the two cavities (9 and 14 Å) in the HMU supramolecular structure. The second cavity has four methyl groups inside that make

Table 1: Specific retention volumes ($V°_{g(T)}$, ml/g) and separation factors α for the D- and L-enantiomers of camphene on the uracil, 5-hydroxy-6-methyluracil and melamine supramolecular net structures based adsorbents

T °C	uracil			HMU			melamine		
	$V°_{g(T)}$		α	$V°_{g(T)}$		α	$V°_{g(T)}$		α
	D	L		D	L		D	L	
40	13.7±0.2	10.0±0.4	1.37±0.07	-	-	-	5.4±0.3	6.3±0.2	1.17±0.10
45	12.6±0.2	8.7±0.4	1.45±0.10	116±1	117.4±0.8	1.01±0.02	2.60±0.06	4.0±0.1	1.54±0.09
50	6.8±0.2	8.0±0.1	1.18±0.06	82.4±0.9	88.9±0.7	1.08±0.02	0.79±0.04	0.99±0.04	1.25±0.11
55	9.8±0.1	9.2±0.4	1.07±0.06	67.7±0.5	65±1	1.04±0.03	2.10±0.09	1.53±0.04	1.37±0.09
60	4.5±0.2	7.0±0.2	1.56±0.1	62±2	61±1	1.02±0.03	0.77±0.03	1.82±0.09	2.36±0.21
65	9.4±0.6	5.7±0.3	1.65±0.19	49±1	47.1±1.4	1.04±0.06	0.41±0.04	0.58±0.03	1.41±0.21
70	6.2±0.2	5.1±0.2	1.22±0.07	37.7±0.9	38.8±0.8	1.03±0.05	0.80±0.02	0.76±0.02	1.05±0.05
75	4.3±0.1	3.0±0.2	1.38±0.14	30.6±0.5	31.6±0.5	1.03±0.03	0.83±0.03	0.92±0.01	1.11±0.05
80	3.1±0.2	3.2±0.2	1.03±0.13	25.7±0.2	25.9±0.5	1.01±0.03	1.52±0.04	0.57±0.01	2.67±0.12

Table 2: Specific retention volumes, ($V°_{g(T)}$, ml/g) and separation factors α for the D- and L-enantiomers of limonene on the uracil, 5-hydroxy-6-methyluracil and melamine supramolecular net structures based solid supports

T °C	uracil			HMU			melamine		
	$V°_{g(T)}$		α	$V°_{g(T)}$		α	$V°_{g(T)}$		α
	D	L		D	L		D	L	
40	26±2	23±3	1.15±0.26	12.9±0.2	14.4±0.6	1.12±0.06	17.3±0.4	12±1	1.47±0.01
45	19.2±0.4	16.5±0.6	1.16±0.06	12±1	11.3±0.4	1.12±0.13	13±1	8.3±0.2	1.53±0.16
50	13±3	10.8±0.1	1.19±0.32	12±1	9.9±0.1	1.19±0.10	7.3±0.6	6.5±0.1	1.12±0.08
55	11.4±0.5	8.7±0.5	1.31±0.14	9.1±0.9	7.8±0.4	1.17±0.18	6.1±0.2	5.6±0.3	1.09±0.09
60	7.3±0.4	6.4±0.4	1.14±0.14	7.1±0.1	7.6±0.2	1.07±0.05	5.5±0.2	4.7±0.2	1.17±0.08
65	5.8±0.4	5.4±0.1	1.07±0.09	6.8±0.3	6.9±0.1	1.01±0.07	4.5±0.3	4.3±0.1	1.05±0.09
70	5.4±0.1	4.8±0.1	1.13±0.04	6.8±0.2	6.3±0.1	1.08±0.04	4.1±0.2	3.9±0.1	1.05±0.04
75	4.8±0.1	4.5±0.1	1.07±0.05	6.4±0.3	5.8±0.1	1.10±0.06	3.8±0.2	3.7±0.1	1.03±0.05
80	4.2±0.1	4.1±0.2	1.02±0.08	5.4±0.2	5.8±0.2	1.07±0.07	3.6±0.2	3.6±0.1	1.00±0.03

it less polar and reduce its real size to approximately 11 Å [52]. In the supramolecular structure of uracil, the cavity dimension is about 7–8 Å [53], and for the melamine supramolecular structure there are no cavities at all [24]. However, in its supramolecular structure six molecules are linked by hydrogen bonds and the seventh molecule is a guest —— linked with other molecules only by weak Van der Waals interactions. Therefore at experimental temperatures the seventh molecule can split out. In that case, a cavity about 5 Å in size can be formed [24]. In both uracil and melamine the cavities are too small to adsorb enantiomers, resulting in the low $V°_{g(T)}$ values. From the phenomena described one can conclude that the capability to separate enantiomers is not connected with the adsorption in the cavities. All of the enantioselectivity was generated by the surface of the supramolecular structure.

Table 3: Specific retention volumes, ($V°_{g(T)}$, ml/g) and separation factors α for the D- and L-enantiomers of camphor on the uracil, 5-hydroxy-6-methyluracil and melamine supramolecular net structures based solid supports

T °C	uracil			HMU			melamine		
	$V°_{g(T)}$		α	$V°_{g(T)}$		α	$V°_{g(T)}$		α
	D	L		D	L		D	L	
45	22.1±0.1	22.7±0.4	1.03±0.02	508±3	525±8	1.04±0.02	-	-	-
50	17.0±0.1	16.5±0.1	1.03±0.01	389±3	379±3	1.03±0.01	33.5±0.4	32.2±0.4	1.04±0.03
55	13.4±0.2	12.9±0.1	1.04±0.02	307±5	296±24	1.04±0.02	11.5±0.3	12.3±0.3	1.07±0.05
60	9.1±0.3	10.3±0.1	1.13±0.05	221±4	240±6	1.04±0.05	10.8±0.2	9.8±0.2	1.10±0.04
65	11.9±0.2	13.0±0.2	1.09±0.03	182±1	180±1	1.01±0.01	9.0±0.3	6.6±0.4	1.36±0.13
70	10.1±0.5	12.9±0.7	1.29±0.15	136±1	134±1	1.02±0.02	8.7±0.4	5.8±0.3	1.50±0.15
75	6.1±0.3	6.3±0.1	1.03±0.06	105±1	103±1	1.02±0.02	5.8±0.1	4.7±0.1	1.23±0.04
80	4.5±0.2	5.2±0.2	1.16±0.08	83±2	82±1	1.01±0.04	4.6±0.2	3.1±0.2	1.48±0.16
85	3.7±0.1	2.3±0.1	1.61±0.09	-	-	-	-	-	-
90	2.9±0.1	2.9±0.1	1.00±0.08	-	-	-	-	-	-
95	1.8±0.1	2.1±0.1	1.17±0.07	-	-	-	-	-	-

For the camphene it is impossible to conclude which of the enantiomers was more strongly adsorbed. At some temperatures D-camphene is better retained than L-camphene, and vice versa. Such phenomena were observed on all three adsorbents. At the same time it is noticeable that at all temperatures D-limonene on the uracil and melamine has stronger retention than L-limonene. On HMU at most temperatures D-limonene was also better retained. For camphor, as for camphene there was no regularity, on uracil the L-enantiomer had slightly better retention, and on melamine the D-enantiomer was better retained. For menthols on all adsorbents L-menthol has the higher $V°_{g(T)}$ value. So all three samples showed similar dependences in enantiomers retention. Apparently the majority of L- or D-isomer retention was determined by enantiomer molecular structure, and not by supramolecular structural properties.

Table 4: Specific retention volumes, ($V°_{g(T)}$, ml/g) and separation factors α for the D- and L-enantiomers of menthol on the uracil, 5-hydroxy-6-methyluracil and melamine supramolecular net structures based solid supports

T, °C	uracil			HMU			melamine		
	$V°_{g(T)}$		α	$V°_{g(T)}$		α	$V°_{g(T)}$		α
	D	L		D	L		D	L	
45	-	-	-	778±7	795±5	1.02±0.02	-	-	-
50	15.2±0,2	29±1	1.94±0.09	584±4	577±8	1.01±0.02	118.2±0.9	119.0±0.8	1.01±0.01
55	10.1±0,3	21±2	2.04±0.26	367±4	438±6	1.19±0.15	39±1	43±1	1.11±0.07
60	15.3±0,2	24±1	1.55±0.11	291±6	319±6	1.10±0.04	46±1	27.7±0.9	1.66±0.10
65	11.0±0,1	12.0±0.2	1.09±0.03	234±8	259±4	1.11±0.05	20.7±0.6	19.5±0.4	1.06±0.05
70	8.1±0,6	19.0±0.1	2.35±0.21	189±2	199±3	1.05±0.02	12.7±0.2	17.3±0.3	1.36±0.05
75	1.3±0,5	19.4±0.3	1.48±0.07	154±2	142±3	1.08±0.04	10.5±0.5	11.9±0.9	1.13±0.14
80	13.3±0,2	16.6±0.9	1.25±0.08	126±1	130±1	1.04±0.02	12.0±0.5	22,0±0,5	1.83±0.11
85	14±2	23.3±0.6	1.66±0.25	-	-	-	4.3±0.3	5.5±0.2	1.28±0.13
90	20.2±0.7	28.5±0.1	1.41±0.11	-	-	-	2.7±0.2	3.0±0.2	1.11±0.14
95	8.9±0.3	8.7±0.4	1.02±0.09	-	-	-	2.8±0.1	2.7±0.2	1.04±0.13
100	-	-	-	-	-	-	2.1±0.1	1.7±0.1	1.24±0.05
105	-	-	-	-	-	-	1.3±0.1	1.5±0.1	1.15±0.15
110	-	-	-	-	-	-	0.65±0,03	0.92±0.04	1.42±0.13

From the tables 1-4 one can note that there is no any temperature dependence of α at all. This phenomenon differs from the observed on conventional CSPs decreasing α with temperature. The explanation of such difference one can find in a great temperature influence on the chiral supramolecular structures [22, 34, 54]. Indeed, unlike chiral molecules, the supramolecular chirality was formed by week noncovalent bonds, such as π-π stacking, hydrogen bond, electrostatic interaction, and coordination. So, any temperature variations may lead to supramolecular structure rearrangement, which results in R- and S- domains ratio changing. The last induce α to spasmodic variations. In some cases retention volumes aren't decrease with temperature decreasing. It also can be linked with supramolecular variations: the cavity accessibility changing with temperature leading additional impact to retention.

3.2. Thermodynamic functions of enantiomer adsorption

In order to calculate differential isosteric internal energies and entropies of adsorption $lnV°_{g(T)}$ vs. 1/T plots were created. In Figure 1 example of such plots is shown. As one can see in the figures, for limonenes in all cases the curve has the bend at 60 °C. Therefore the thermodynamic functions of adsorption in such cases were calculated on the linear sections. It must be noted that for menthol on uracil and camphene on melamine, the observed plots do not allow selection of a reliable linear section, therefore thermodynamic functions of adsorption were not calculated.

In Tables 5–7 the $-\Delta U$ and $-\Delta S$ of enantiomer adsorption on the adsorbents studied are shown. As one can see from Table 5, for camphene and camphor the energies and entropies of enantiomer adsorption on uracil were noticeably different. Thus, for

camphenes, $-\Delta U$ and $-\Delta S$ vary almost by a factor of two. For limonene in the temperature range 40–60 °C the thermodynamic features of adsorption were not different, whereas in the temperature range 60–80 °C $-\Delta U$ and $-\Delta S$ for the L- and D-enantiomers were different. It is interesting to note that on the different linear sections of $lnV^{\circ}_{g(T)}$ vs. 1/T dependence the values of the thermodynamic functions vary by more than twice, and at the lowest temperatures the energy and entropy of adsorption were higher.

On HMU in many cases the difference between the thermodynamic functions for L- and D-enantiomers was within the limits of experimental error. Only for menthol and camphor in the temperature range 60–80 °C $-\Delta U$ and $-\Delta S$ vary reliably. This is probably because of the smaller separation factors for enantiomers on HMU. Also, similarly with the previous adsorbent, at high temperatures $-\Delta U$ and $-\Delta S$ of adsorption were smaller then at low temperatures. In any case this difference was outside of the limits of experimental error.

Due to high enantioselectivity, on melamine in all cases a significant difference in $-\Delta U$ and $-\Delta S$ of enantiomer adsorption was observed. In some cases it amounted to 20–30 kJ/mol. For limonenes $-\Delta U$ and $-\Delta S$ of adsorption in the temperature range 40–50 °C were approximately three times greater than in the temperature range 50–80 °C.

It can be concluded that the enantioselectivity of the adsorbents tested in this work was governed by the difference in internal energy and entropy of enantiomer adsorption on the supramolecular structure surface. If $lnV^{\circ}_{g(T)}$ vs. 1/T plots have any bends, $-\Delta U$ and $-\Delta S$ values at lower temperature were significantly greater than at higher temperatures.

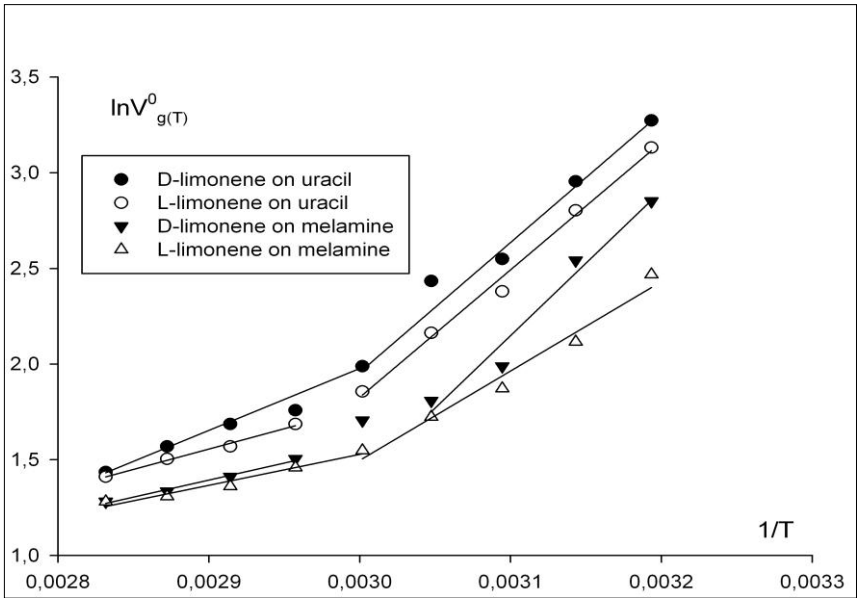

Figure 1: $\ln V^{\circ}_{g(T)}$ vs. 1/T dependence for D- and L-limonene on the uracil and melamine based adsorbent.

Table 5: Differential isosteric internal energy of adsorption (−ΔU, kJ/mol), entropy parameter of adsorption (−ΔS, J/(mol K)) and linear regression coefficients r for camphene, limonene and camphor on the adsorbent, based on the supramolecular structure of uracile

	limonene						camphor		camphene	
	D	L	D	L	D	L	D	L	D	L
-ΔU	43±3	40±4	26.9±0.7	18±1	56±3	55±3	51±5	39±3	73±2	39±2
-ΔS	111±9	103±11	63±2	38±4	153±8	151±8	126±14	88±8	190±6	101±7
r	0.9824	0.9735	0.9993	0.9949	0.9981	0.9964	0.9923	0.9925	0.9992	0.9946
T range ˚C	40-80		60-80		40-60		45-60	45-75	65-80	55-80

Table 6: Differential isosteric internal energy of adsorption (−ΔU, kJ/mol), entropy parameter of adsorption (−ΔS, J/(mol K)) and linear regression coefficients r for camphene, limonene, camphor and menthol on the adsorbent, based on the supramolecular structure of HMU

	limonene				menthol			
	D	L	D	L	D	L	D	L
-ΔU	-	34±3	-	17.4±0.2	65±10	53±1	41±0	44±1
-ΔS	-	85±8	-	35.2±0.3	149±29	112±4	77±0	85±4
r	-	0.9939	-	0.9998	0.9895	0.9995	0.9999	0.9992
T range, ˚C	-	40-55	-	60-75	45-55		60-80	
	camphene				camphor			
	D	L	D	L	D	L	D	L
-ΔU	47±7	51±2	44±2	41±0.8	44±1	46±3	49±2	53±1
-ΔS	108±21	121±7	97±4	89±3	85±4	93±9	102±5	114±3
r	0.9894	0.9991	0.9983	0.9997	0.9997	0.9964	0.9982	0.9994
T range, ˚C	45-55		60-80		45-55		60-80	

Table 7: Differential isosteric internal energy of adsorption (−ΔU, kJ/mol), entropy parameter of adsorption of adsorption (−ΔS, J/(mol K)) and linear regression coefficients r for limonene, camphor and menthol on the adsorbent, based on the supramolecular structure of melamine

	limonene						menthol		camphor	
	D	L	D	L	D	L	D	L	D	L
-ΔU	35±4	26±3	72±13	50±5	23±2	13±2	92±6	64±4	37±4	47±4
-ΔS	91±12	65±9	207±39	140±15	55±5	28±5	237±17	155±12	83±10	113±12
r	0.9530	0.9618	0.9854	0.9954	0.9866	0.9804	0.9928	0.9918	0.9866	0.9886
temperature range, ˚C	40-80		40-50		50-80		40-80		55-80	55-75

3.3. Enantiomer separation

The separation on the adsorbents studied was followed by too much peak broadening leading to poor separation. For these reasons, uracil was impregnated on Carbopack C adsorbent, and melamine was impregnated on Polysorb-1 adsorbent. The 2-butanol racemate was used. The typical separation was shown on Fig. 2 (Carbopack C with 1% of uracil, T=130 ˚C, α=1.12, R=0.22). The best separation was obtained at 150 ˚C on Polysorb-1 with 5% of melamine (Fig. 3, α=3.01, R=2.65).

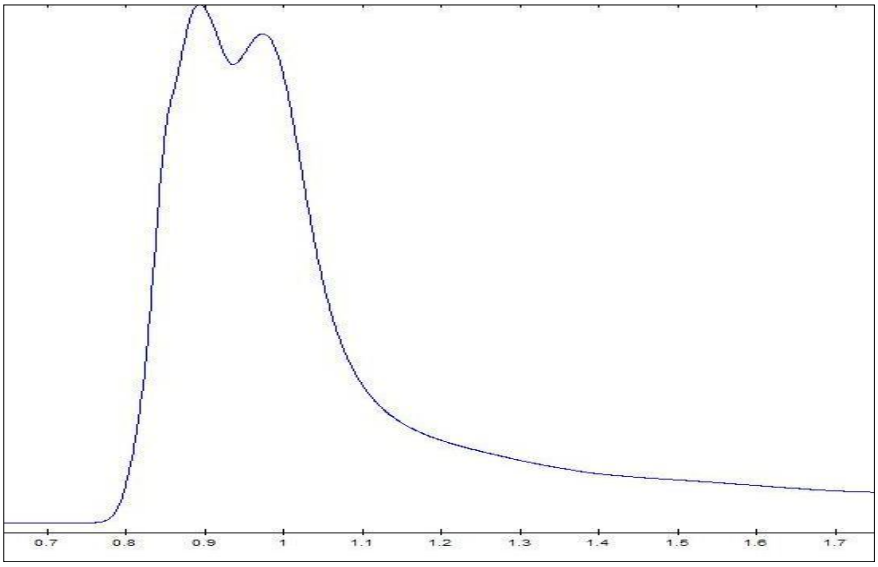

Figure 2: The separation of butanol-2 enantiomers on Carbopack C with 1% of uracil at 130 ˚C

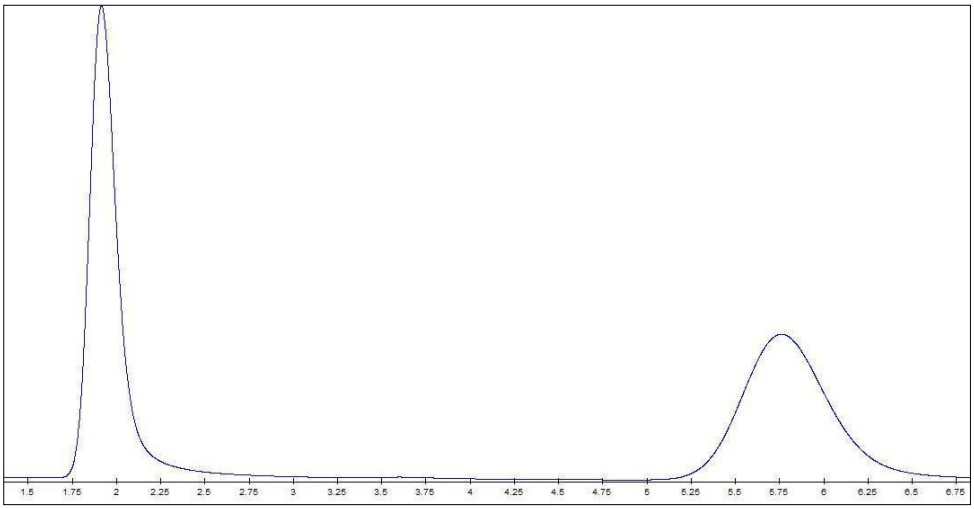

Figure 3: The separation of butanol-2 enantiomers on Polysorb-1 with 5% of melamine at 150 ˚C

3.4. The reasons for the observed enantioselectivity

From 4.2 it is clear, that enantioselectivity was caused by the difference in the internal energy and entropy of enantiomer adsorption on the supramolecular structure surface. For this, the number of R- and S-homochiral domains shouldn't be equal. In can be caused by two reasons: the described above spontaneous mirror-symmetry breaking or the presence of external chirality source. There is no polarized light, optically pure solvent or any other optically pure substance. But during the evaporation, the aqueous solution of modifiers has been rapidly stirred. Due to the fact, that the supramolecular structures formed by week hydrogen bonding, the sum of thermal motion energy and kinetic energy of stirring at 60 ˚C (evaporation temperature) is quite sufficient to breaking H-bond and spinning supramolecular structure in one direction.

To prove this suggestion an additional experiment has been conducted: the porous polymer Polysorb-1 was modified by melamine at very slow stirring (the melamine aqueous solution has been preliminary stirred well), packed in 1m column and then tested for enantioselectivity. No enantioselectivity was observed. Consequently, the enantioselectivity on the samples studied is caused by stirring.

CONCLUSION

It was determined that the supramolecular structures of uracil, HMU and melamine can separate camphene, limonene, camphor and menthol enantiomers with relatively high separation factors. The enantioselectivity of such supramolecular structures was linked with the difference in internal energies and entropies of enantiomer adsorption on the supramolecular structure surface. After depth analysis of the data obtained the fundamental reason leading to enantiomers separations is the excess of one of the chiral domains in modifiers 2D supramolecular structures, caused by intensive stirring during the modification. Yet nowadays there is no reliable method to determine the macroscopic chirality of 2D-supramolecular structures, so the gas chromatography was prove to be capable to do it.

The chiral surfaces obtained can be used in chemical sensors to reach the necessarily sensitivity and selectivity.

ACKNOWLEDGMENTS

The financial support of the Russian Science Foundation (grant 16-13-10257) is gratefully acknowledged.

REFERENCES

[1] Dretschkow, T., Dakkouri, A. S., Wandlowski, T., 1997, "In-situ scanning tunneling microscopy study of uracil on Au(111) and Au(100)," Langmuir, 13, pp. 2843-2856.

[2] Cavallini, M., Aloisi, G., Bracali, M., Guidelli, R., 1998, "An in situ STM investigation of uracil on Ag(111)," J. Electroanal. Chem. , 444, pp. 75–81.
[3] Li, W.-H., Haiss, W., Floate, S., Nichols, R. J., 1999, "In-situ infrared spectroscopic and scanning tunneling microscopy investigations of the chemisorption phases of uracil, thymine, and 3-methyl uracil on Au(111) electrodes," Langmuir, 15, pp. 4875-4883.
[4] Kos´cielski, T., Sybilska, D., Jurczak, J., 1983, "Separation of α- and β-pinene into enantiomers in gas-liquid chromatography systems via α-cyclodextrin inclusion complexes," J. Chromatogr. , 280, pp. 131–134.
[5] Mosinger, J., Tomankova, V., Nemcova, I., Zyka, J., 2001, "Cyclodextrins in analytical chemistry," Anal. Lett., 34, pp. 1979-2004.
[6] Aboul-Enein, H. Y., Stefan, R.-I., 1998, "Enantioselective sensors and biosensors in the analysis of chiral drugs," Critical Reviews in Analytical Chemistry, 28, pp. 259–266.
[7] Chen, Y., Huang, Y., Guo, D., Chen, C., Wang, Q., Fu, Y., 2014, "A chiral sensor for recognition of DOPA enantiomers based on immobilization of β-cyclodextrin onto the carbon nanotube-ionic liquid nanocomposite," J Solid State Electrochem, 18, pp. 3463–3469.
[8] Schurig, V., 2001, "Separation of enantiomers by gas chromatography," Journal of Chromatography A, 906, pp. 275–299.
[9] Zhou, J., Tang, J., Tang, W., 2015, "Recent development of cationic cyclodextrins for chiral separation," Trends in Analytical Chemistry 65, pp. 22-29.
[10] Weatherly, C. A., Na, Y.-C., Nanayakkara, Y. S., 2014, "Reprint of: Enantiomeric separation of functionalized ethano-bridged Tröger bases using macrocyclic cyclofructan and cyclodextrin chiral selectors in high-performance liquid chromatography and capillary electrophoresis with application of principal component analysis," J. Chromatogr. B 968, pp. 40–48.
[11] Al-Hussin, A., Boysen, R. I., Saito, K., 2014, "Preparation and electrochromatographic characterization of new chiral β-cyclodextrin poly(acrylamidopropyl) porous layer open tubular capillary columns," J. Chromatogr. A, 1358, pp. 199–207.
[12] Huang, G., Ou, J., Zhang, X., 2014, "Synthesis of novel perphenylcarbamated β-cyclodextrin based chiral stationary phases via thiol-ene click chemistry," Electrophoresis, 35, pp. 2752-2758.
[13] Pang, L., Zhou, J., Tang, J., 2014, "Evaluation of perphenylcarbamated cyclodextrin clicked chiral stationary phase for enantioseparations in reversed phase high performance liquid chromatography," J. Chromatogr. A 1363, pp. 119-127
[14] Zhang, J.-H., Xie, S.-M., Zhang, M., 2014, "Novel inorganic mesoporous material with chiral nematic structure derived from nanocrystalline cellulose for high-resolution gas chromatographic separations," Anal. Chem. , 86, pp. 9595–9602.

[15] Kapnissi-Christodoulou, C. P., Stavrou, I. J., Mavroudi, M. C., 2014, "Chiral ionic liquids in chromatographic and electrophoretic separations," J. Chromatogr. A 1363, pp. 2-10.
[16] Kulsing, C., Knob, R., Macka, M., 2014, "Molecular imprinted polymeric porous layers in open tubular capillaries for chiral separations," J. Chromatogr. A 1354, pp. 85–91.
[17] Ahmed, M., Yajadda, M. M. A., Han, Z. J., 2014, "Single-walled carbon nanotube-based polymer monoliths for the enantioselective nano-liquid chromatographic separation of racemic pharmaceuticals," J. Chromatogr. A 1360, pp. 100–109
[18] Meijer, E. W., Palmans, A. R. A., 2007, "Amplification of chirality in dynamic supramolecular aggregates," Angewandte Chemie International Edition, 46, pp. 8948 – 8968.
[19] Fujiki, M., 2014, "Supramolecular chirality: solvent chirality transfer in molecular chemistry and polymer chemistry," Symmetry 6, pp. 677-703.
[20] Bruin, A. G. d., Barbour, M. E., Briscoe, W. H., 2014, "Macromolecular and supramolecular chirality: a twist in the polymer tales," Polymer International 63, pp. 165–171.
[21] Zhao, L., Liu, M., Li, S., Li, A., An, H., Ye, H., Zhang, Y. J., 2015, "Aggregation and supramolecular chirality of 5,10,15,20-tetrakis-(4-sulfonatophenyl)-porphyrin on an achiral poly(2-(dimethylamino)ethyl methylacrylate)-grafted ethylene-vinyl alcohol membrane," Material Chemistry C, 3, pp. 3650-3658.
[22] Zhang, L., Qin, L., Wang, X., Cao, H., Liu, M., 2014, "Supramolecular chirality in self-assembled soft materials: regulation of chiral nanostructures and chiral functions," Advanced Materials 26, pp. 6959–6964.
[23] Gardener, J. A., Shvarova, O. Y., Briggs, G. A. D., Castell, M. R., 2010, "Intricate hydrogen-bonded networks: binary and ternary combinations of uracil, PTCDI, and melamine," J. Phys. Chem. C, 114, pp. 5859–5866.
[24] Zhang, H.-M., Xie, Z.-X., Long, L.-S., Zhong, H.-P., Zhao, W., Mao, B.-W., Xu, X., Zheng, L.-S., 2008, "One-step preparation of large-scale self-assembled monolayers of cyanuric acid and melamine supramolecular species on Au(111) surfaces," J. Phys. Chem. C, 112, pp. 4209-4218.
[25] Wang, Y., Zhou, D., Li, H., Li, R., Zhong, Y., Sun, X., Sun, X., 2014, "Hydrogen-bonded supercoil self-assembly from achiral molecular components with light-driven supramolecular chirality," J. Mater. Chem., 2, pp.
[26] Vera, F., Serrano, J. L., Santo, M. P. D., Barberi, R., Rosa, M. B., Sierra, T., 2012, "Insight into the supramolecular organization of columnar assemblies with phototunable chirality," J. Mater. Chem., 22, pp. 18025–18032.
[27] Sun, X., Jonkman, H. T., Silly, F., 2010, "Tailoring two-dimensional PTCDA–melamine self-assembled architectures at room temperature by tuning molecular ratio," Nanotechnology, 21, pp. 165602.

[28] Silly, F., Shaw, A. Q., Castell, M. R., Briggs, G. A. D., 2008, "A chiral pinwheel supramolecular network driven by the assembly of PTCDI and melamine," Chem. Commun., pp. 1907–1909. DOI DOI: 10.1039/b715658h

[29] Wang, K.-R., Han, D., Cao, G.-J., Li, X.-L., 2015, "Synthesis and predetermined supramolecular chirality of carbohydrate-functionalized perylene bisimide derivatives," Chemical Asian Journal 10, pp. 1204 – 1214.

[30] Shen, Z., Wang, T., Liu, M., 2014, "Macroscopic chirality of supramolecular gels formed from achiral tris(ethyl cinnamate) benzene-1,3,5-tricarboxamides," Angewandte Chemie International Edition, 53, pp. 13424 –13428.

[31] Cano, M., Sanchez-Ferrer, A., Serrano, J. L., Gimeno, N., Ros, M. B., 2014, "Supramolecular architectures from bent-core dendritic molecules," Angewandte Chemie International Edition, 53, pp. 13449 –13453.

[32] Sasaki, T., Ida, Y., Hisaki, I., Yuge, T., Uchida, Y., Tohnai, N., Miyata, M., 2014, "Characterization of supramolecular hidden chirality of hydrogen-bonded networks by advanced graph set analysis," Chemical European Journal 20, pp. 2478 – 2487.

[33] Dryzun, C., Avnir, D., 2012, "On the abundance of chiral crystals," Chemical Communications, 48, pp. 5874 –5876.

[34] Mineo, P., Villari, V., Scamporrinoa, E., Micalib, N., 2014, "Supramolecular chirality induced by a weak thermal force," Soft Matter 10, pp. 44–47.

[35] Lin, J., Guo, Z., Plas, J., Amabilino, D. B., Feyter, S. D., Schenning, A. P. H. J., 2013, "Homochiral and heterochiral assembly preferences at different length scales – conglomerates and racemates in the same assemblies," Chemical Communications 49, pp. 9320-9322.

[36] P.Chen, Ma, X., Hu, K., Rong, Y., Liu, M., 2011, "Left or right? The direction of compression-generated vortex-like flow selects the macroscopic chirality of interfacial molecular assemblies," Chemical European Journal 17, pp. 12108 – 12114.

[37] Azeroual, S., Surprenant, J., Lazzara, T. D., Kocun, M., Tao, Y., Cuccia, L. A., Lehn, J.-M., 2012, "Mirror symmetry breaking and chiral amplification in foldamer-based supramolecular helical aggregates," Chemical Communications 48, pp.

[38] Sun, K., Shao, T.-N., Xie, J.-L., Lan, M., Yuan, H.-K., Xiong, Z.-H., Wang, J.-Z., Liu, Y., Xue, Q.-K., 2012, "Chiral pinwheel clusters lacking local point chirality," Small, 8, pp. 2078–2082.

[39] Katsonis, N., Xu, H., Haak, R. M., Kudernac, T., Tomovic, Z., George, S., Auweraer, M. V. d., Schenning, A. P. H. J., Meijer, E. W., Feringa, B. L., Feyter, S. D., 2008, "Emerging solvent-induced homochirality by the confinement of achiral molecules against a solid surface," Angewandte Chemie International Edition 47, pp. 4997 –5001.

[40] Asano, N., Harada, T., Sato, T., Tajimac, N., Kuroda, R., 2009, "Supramolecular chirality measured by diffuse reflectance circular dichroism spectroscopy," Chemical Communications 45, pp. 899–901.
[41] Tejedor, R. M., Oriol, L., Serrano, J. L., Ureña, F. P., González, J. J. L., 2007, "Photoinduced chiral nematic organization in an achiral glassy nematic azopolymer," Advanced Functional Materials 17, pp. 3486–3492.
[42] Zhang, Y., Chen, P., Liu, M., 2008, "General method for constructing optically active supramolecular assemblies from intrinsically achiral water-insoluble free-base porphyrins," Chemical European Journal 14, pp. 1793 – 1803.
[43] Ikbal, S. A., Brahma, S., Rath, S. P., 2014, "Transfer and control of molecular chirality in the 1 : 2 host–guest supramolecular complex consisting of Mg(II)bisporphyrin and chiral diols: the effect of H-bonding on the rationalization of chirality," Chemical Communications 50, pp. 14037-14040.
[44] Imai, Y., Shiota, N., Kinuta, T., Okuno, T., Nakano, Y., Harada, T., Sato, T., Fujiki, M., Kuroda, R., Matsubara, Y., 2010, "A 2D layered chiral supramolecular organic fluorophore composed of 1-amino-2-indanol and carboxylic acid derivatives," European Journal of Organic Chemistry pp. 1353–1357.
[45] Matassa, R., Carbone, M., Lauceri, R., Purrello, R., Caminiti, R., 2007, "Supramolecular structure of extrinsically chiral porphyrin hetero-assemblies and achiral analogues," Advanced Materials 19, pp. 3961–3967.
[46] Ruiz, U., Pagliusi, P., Provenzano, C., Shibaev, V. P., Cipparrone, G., 2012, "Supramolecular chiral structures: smart polymer organization guided by 2D polarization light patterns," Advanced Functional Materials 22, pp. 2964–2970.
[47] Ohta, E., Sato, H., Ando, S., Kosaka, A., Fukushima, T., Hashizume, D., Yamasaki, M., Hasegawa, K., Muraoka, A., Ushiyama, H., Yamashita, K., Aida, T., 2010, "Redox-responsive molecular helices with highly condensed π-clouds," Nature Chemistry, 3, pp. 68–73.
[48] Morf, P., Ballav, N., Putero, M., 2010, "Supramolecular structures and chirality in dithiocarbamate self-assembled monolayers on Au(111)," J. Phys. Chem. Lett. , 1, pp. 813–816.
[49] Böhringer, M., Schneider, W.-D., Berndt, R., 2000, "Two-dimensional self-assembly of supramolecular structures," Surf. Rev. Lett. , 7, pp. 661–666.
[50] Tang, L., Li, F. S., Guo, Q., 2013, "Complete structural phases for self-assembled methylthiolate monolayers on Au(111)," J. Phys. Chem. C 117, pp. 21234–21244.
[51] Petit-Garrido, N., Ignés-Mullol, J., Claret, J., 2009, "Chiral selection by interfacial shearing of self-assembled achiral molecules," Phys. Rev. Lett., 103, pp. 237802.
[52] Gus'kov, V. Y., Gainullina, Y. Y., Ivanov, S. P., Kudasheva, F. K., 2014, "Thermodynamics of organic molecules adsorption on modified by 5-

hydroxy-6-methyluracil sorbents by inverse gas chromatography," J. Chromatogr. A 1356, pp. 230–235.

[53] Gus'kov, V. Y., Gainullina, Y. Y., Ivanov, S. P., Kudasheva, F. K., 2014, "Porous polymer adsorbents modified with uracil," Protection of Metals and Physical Chemistry of Surfaces 50, pp. 55–58.

[54] Yang, Y., Zhang, Y., Wei, Z., 2013, "Supramolecular helices: chirality transfer from conjugated molecules to structures," Advanced Materials 25, pp. 6039–6049.